Damage prediction of composite plate for structural health monitoring

Tomáš Kroupa[1]*, Robert Zemčík[2], Vladislav Laš[3] and Milan Růžička[4]

[1]* Faculty of Applied Sciences, Department of Mechanics, University of West Bohemia, Univerzintí 8, 306 14, Plzeň, Czech Republic, tel.: +420 377 63 2367, fax.: +420 377 63 2302, e-mail: kroupa@kme.zcu.cz

[2] Faculty of Applied Sciences, Department of Mechanics, University of West Bohemia, Univerzintí 8, 306 14, Plzeň, Czech Republic, tel.: +420 377 63 2336, fax.: +420 377 63 2302, e-mail: zemcik@kme.zcu.cz

[3] Faculty of Applied Sciences, Department of Mechanics, University of West Bohemia, Univerzintí 8, 306 14, Plzeň, Czech Republic, tel.: +420 377 63 2301, fax.: +420 377 63 2302, e-mail: las@kme.zcu.cz

[4] Czech Technical University in Prague, Technická 4, 166 07 Praha 6, Czech Republic, tel.: +420 224 352 512, fax.: +420 233 322, e-mail milan.ruzicka@fs.cvut.cz

ABSTRACT

In order to increase the safety and reliability of composite structures it is important that the structural health monitoring system has certain feature, such as the ability to identify the location and scope of impact, to analyze whether failure occurs, and eventually to asses the residual strength. The work focuses on the experimental and numerical analysis of unidirectional composite plate made of carbon fibers and epoxy resin subjected to random low velocity impact loading caused by a projectile. An array of sensors is attached to the opposite side of the plate and the corresponding strain dependencies are recorded during experiment. The goal is to identify the location of impact and the character of the induced force. The location of impact is assessed using the knowledge of velocities of waves traveling in all directions and finite element analysis in combination with mathematical optimization. The results of the numerical solution are then used in failure analysis. The failure analysis is utilizing the Puck's criterion to predict the occurrence of failure. The mathematical model of wave propagation was validated by experiment.

Keywords: Impact, identification, stress waves, failure, composite

1. INTRODUCTION

The trends in design of modern structures call for the application of so-called smart materials which leads in the construction of smart, adaptive or intelligent structures. The main feature of such smart structure is to mimic biological functions, i.e., the system (consisting of sensors, controller and actuators) responds to external stimuli, adapts to surrounding conditions, or it can even learn.

One application filed is the structural health monitoring (SHM) which enables to monitor, assess, adapt or eventually repair the current state [1, 7]. The reasons for the usage are mainly the safety, lifetime elongation or performance increase. The main phases of SHM can be described as detection of failure, localization, assessment of size or orientation, estimation of risk (residual strength and lifetime), and eventually healing. As this process can be fully embedded, automated and operating in real-time, substantial cost savings can be made since there is reduced need for additional off-line service maintenance using standard inspection procedures with nondestructive techniques (NDT). The disadvantages of classical procedures are human labor and that the damage site would have to be accessible and known a priori [3].

2. PROBLEM FORMULATION

The goal of the work is to identify the location of impact of glass spherical projectile on unidirectional composite plate. The plate is made from four carbon-epoxy prepregs and is clamped along the edges (see Figure 1 for details). There were seven semiconductor strain gauges (6 mm effective length) glues on the rear side of the plate. The signals were amplified and recorded by pair of oscilloscopes (see Figure 2) in terms of strain rates. The signals were then filtered (see Figure 3), synchronized and averaged from multiple tests (see Figure 4).
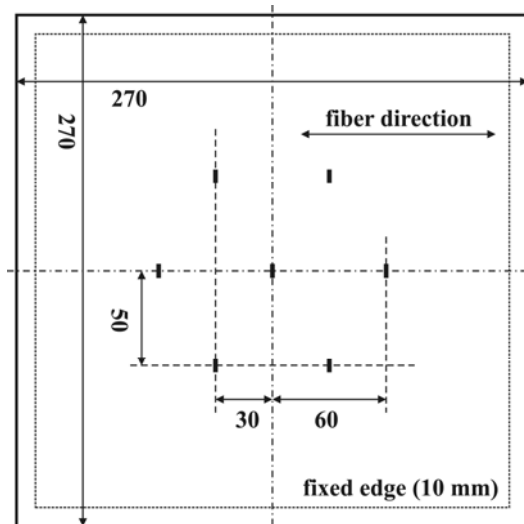

Figure 1. Composite plate with strain gauges.

Simple tensile tests were performed in order to determine mechanical properties of the plate. The tests were performed on specimens for three fiber directions (0°, 45°, 90°). The moduli corresponding to material axes (L – longitudinal or fiber direction, T – transverse) were identified by comparing results of FEA and experiment. The non-linear stress-strain relation was used within the identification process with the use of the gradient method [6]. Force-displacement diagram is shown in the Figure 5.
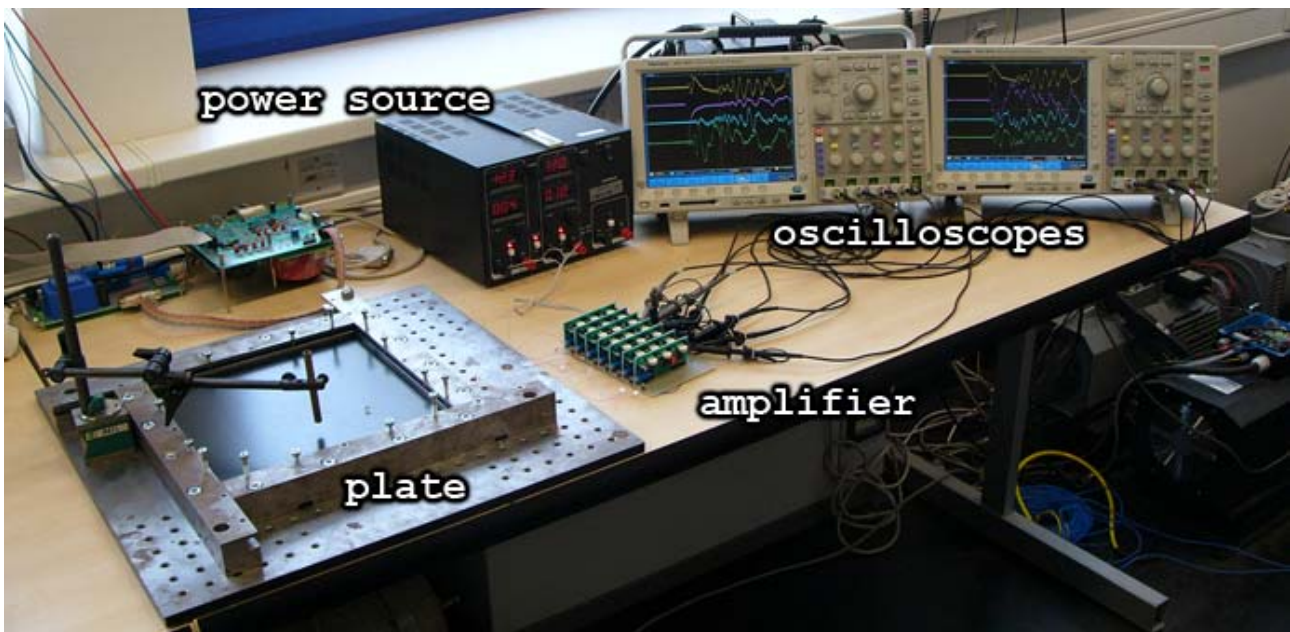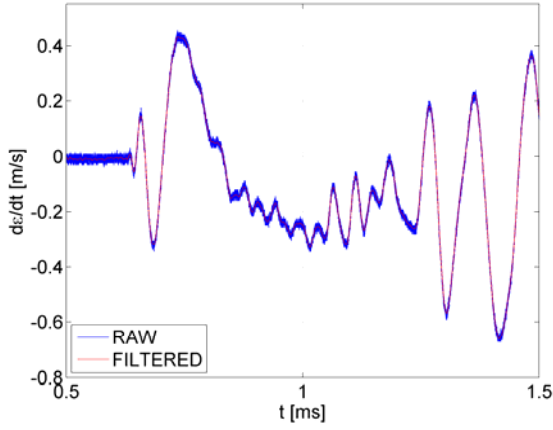

Figure 2. Experimental setup.
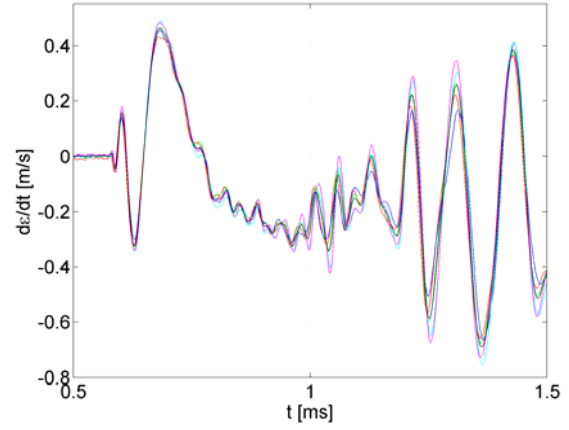
Figure 3. Raw and filtered signals.

Figure 4. Synchronized signals from multiple experiments.
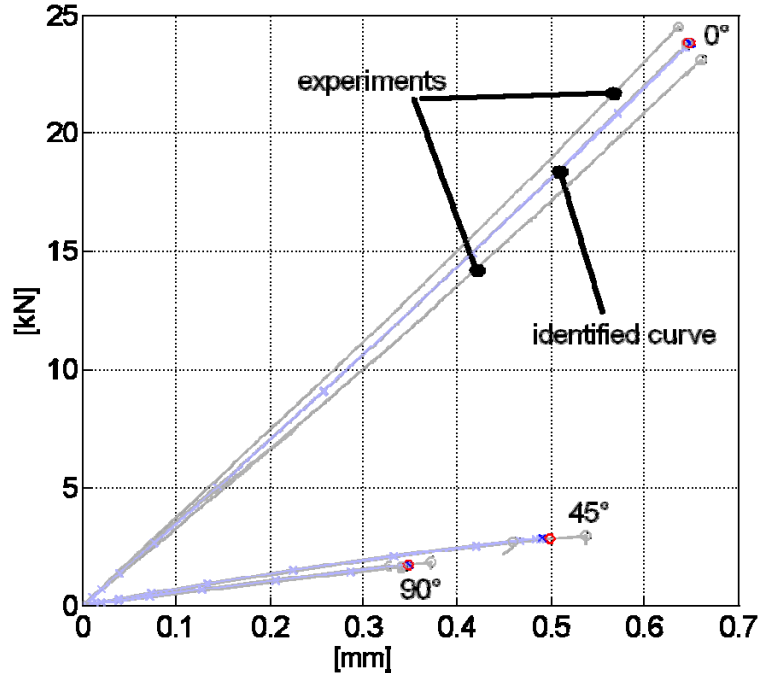

Figure 5. Force-displacement diagrams and results of the identification process.

Moduli were taken as tangent of the stress-strain curves for zero strain. Poisson's ratio was identified separately using two perpendicular strain gauges. Both tensile strengths X^{T} and Y^{T} and shear strength S^{L} were identified using Puck's action plane concept [9]. Linear stress-strain relation for transverse isotropic material in plane stress state [2] is used for further analyses in the form

$$
\begin{bmatrix} \sigma_{\mathrm{L}} \\ \sigma_{\mathrm{T}} \\ \tau_{\mathrm{LT}} \end{bmatrix} = \begin{bmatrix} \dfrac{E_{\mathrm{L}}}{(1-\nu_{\mathrm{LT}}\nu_{\mathrm{TL}})} & \dfrac{\nu_{\mathrm{LT}}E_{\mathrm{T}}}{(1-\nu_{\mathrm{LT}}\nu_{\mathrm{TL}})} & 0 \\ \dfrac{\nu_{LT}E_{T}}{(1-\nu_{\mathrm{LT}}\nu_{\mathrm{TL}})} & \dfrac{E_{T}}{(1-\nu_{\mathrm{LT}}\nu_{\mathrm{TL}})} & 0 \\ 0 & 0 & G_{\mathrm{LT}} \end{bmatrix} \begin{bmatrix} \varepsilon_{\mathrm{L}} \\ \varepsilon_{\mathrm{T}} \\ \gamma_{\mathrm{LT}} \end{bmatrix}, \quad \nu_{\mathrm{TL}} = \nu_{\mathrm{LT}}\dfrac{E_{\mathrm{T}}}{E_{\mathrm{L}}}. \tag{1}
$$

The values and meanings of used constants are given in Table 1.

Table 1. Mechanical properties and dimensions of the plate and projectile.

Plate – carbon/epoxy composite	
E_L – Young's modulus in fiber direction [GPa]	107.95
E_T – Young's modulus in transverse direction [GPa]	7.59
G_{LT} – Shear modulus [GPa]	4.08
ν_{LT} – Poisson's ratio [-]	0.3225
X^T – Tensile strength in fiber direction [MPa]	1190
X^C – Compressive strength in fiber direction [MPa]	1170
Y^T – Tensile strength in transverse direction [MPa]	43
Y^C – Compressive strength in transverse direction [MPa]	200
S^L – Shear strength	62
ρ_c – Density of the composite [kg/m^3]	1468
$d \times d$ – Dimensions of the oscillating plate [mm] × [mm]	250 × 250
h – Thickness of the plate [mm]	0.85
Sphere – glass	
E_g – Young's modulus [GPa]	70
ν_g – Poisson's ratio [-]	0.25
ρ_g – Density [kg/m^3]	2551.6
m_g – Mass [g]	0.167
D – Diameter [mm]	5

3. IDENTIFICATION OF IMPACT POSITION

Two tested methods for the identification are described below. The first method tested for the identification of impact location can be denoted as the ray or peak-peak method. The latter method uses finite element analysis (FEA) in MSC.Marc code for the simulation of the non-stationary state of the plate and optimization techniques of optiSLang code.

3-1. RAY METHOD

As the material is orthotropic the velocity of the signal peak across the plate is direction dependent. For simplicity we assume that the velocity v of propagation is such that the envelope of disturbed area is an ellipsoid with axes parallel to material principal directions L and T. Therefore, the identification of impact location [x, y] (measured from the center) means to minimize the residual

$$r = \sum_{i=1}^{7}\left\{\left(\sqrt{dx^2 + dy^2} - v \cdot dt\right)^2\right\} \qquad (2)$$

with

$$dx = x - x_i^G, \; dy = y - y_i^G, \; dt = t_i - t_s, \; v = v(v_L, v_T, dx, dy) \qquad (3)$$

x_i^G and y_i^G being the coordinates of i-th strain gauge, t_i is time at which the peak arrives to i-th strain gauge and t_s is the unknown time shift of all experimental signals. The axial velocities $v^L = 566$ m/s and $v^T = 401$ m/s were identified from test when the impact was at the central strain gauge. The peaks' arrivals were taken as times when the signal $s_{EXP}^i(t)$ reached the trigger value

$$T_{\text{EXP}}^{i} = \underset{t}{\text{avg}}\left(\left|s_{\text{EXP}}^{i}(t)\right|\right),\tag{4}$$

where "avg" denotes the averaged value of the signal.

The method was implemented in Matlab while the minimum of the residual r was found by calculating all combination within given ranges of x, y and t_s. The example of results for impact at location $[x, y] = [50, 50]$ mm is shown in Figure 6. The yellow ellipses denote the envelopes of disturbed areas of back propagating signal, the blue square denotes the maximum estimated error in peaks' traveled distances, and the purple lines connect impact location with strain gauges.
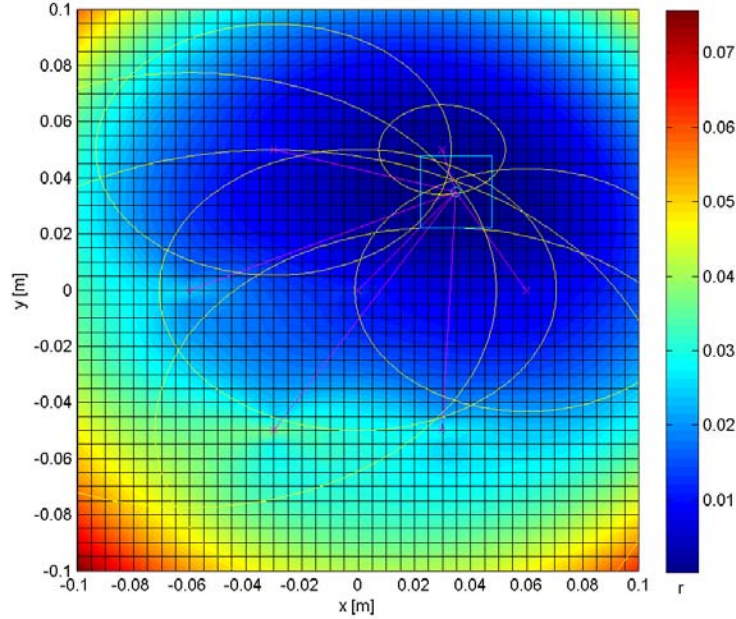

Figure 6. Example of residual contours and identified location (blue circle) for impact at $[x, y] = [50, 50]$ mm.

3-2. FEA BASED METHOD

The combination of FEA, Matlab and optimization software was used. The optiSLang software controlled the process of optimization, i.e. it estimated the impact location, while the MSC.Marc code calculated the signals from strain gauge positions. It used shell elements (edge length $a = 5$ mm) and single-step Houbolt integration scheme. The Matlab code generated necessary input/output files and processed and compared the signals.

Several techniques for comparison of experimental and FEA results were tested. In order to speed up the technique selection process a database of signals for all possible locations (within 150×150 mm which equals 31×31 a) around the center of the plate) and different impact velocities was pre-calculated, so that the optimization could be performed on this virtual problem. The method providing the best results is described below.

Triggers of signals are calculated from relation (4) and from

$$T_{\text{FEA}}^{i} = \underset{t}{\text{avg}}\left(\left|s_{\text{FEA}}^{i}(t)\right|\right) \cdot \left[\frac{t_{\text{FEA}}^{\max}}{t_{\text{EXP}}^{\max}}\right],\tag{5}$$

where $s_{\text{FEA}}^{i}(t)$ is the signal obtained from finite element analysis, and $t_{\text{EXP}}^{\max}$ and $t_{\text{FEA}}^{\max}$ means the length of the signals. Times $\Delta t_{\text{EXP}}^{i}$ and $\Delta t_{\text{FEA}}^{i}(\delta)$ when the triggers were reached are determined with the knowledge of the values of the triggers (see Figure 7). If the T_{EXP} is positive (resp. negative) T_{FEA} is searched also as positive (resp. negative). The difference between signals from i-th strain gauge is calculated as

$$\Delta t^{i}(\delta) = \left[\Delta t_{EXP}^{i} - \Delta t_{FEA}^{i}(\delta)\right]^{2}. \tag{6}$$
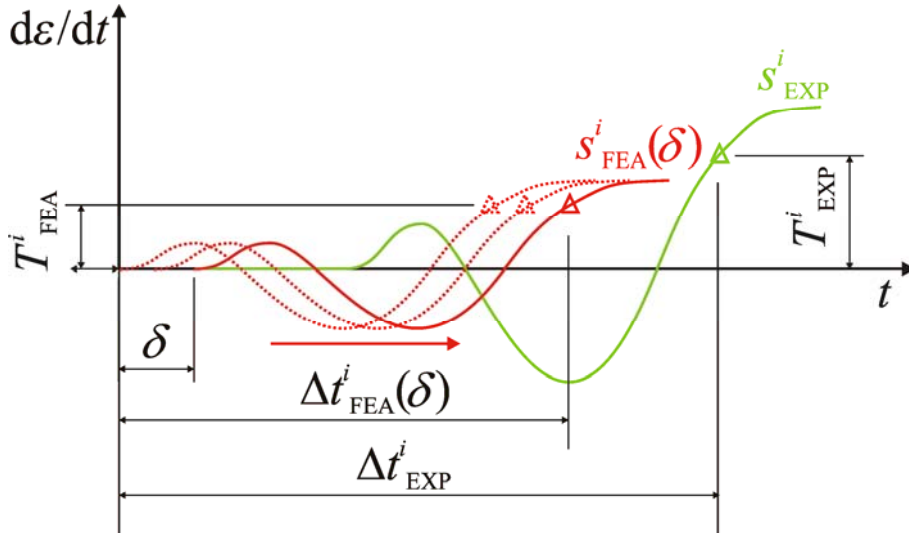

Figure 7. Illustration of the signals characteristics.

Signals difference from all strain gauges is calculated as sum

$$\Delta t(\delta) = \sum_{i} \Delta t^{i}(\delta). \tag{7}$$

The residual could be calculated now as $r = \min_{\delta}\left[\Delta t(\delta)\right]$. Nevertheless, this approach is not capable to avoid problems with situation when the impact in FEA analysis is near strain gauge. This impact produces signal with large amplitude and in often case with overbalanced deflection only with positive or negative values. When the trigger in experiment is found positive and deflection of FEA signal is negative, the trigger does not work well and large residual is calculated. Therefore, the residual is calculated as minimum from residuals calculated as (see Figure 8)

$$r = \min_{i}[r^{i}], \quad \text{where} \quad r^{i} = \min_{\delta}\left[\Delta t(\delta) - \Delta t^{i}(\delta)\right]. \tag{8}$$
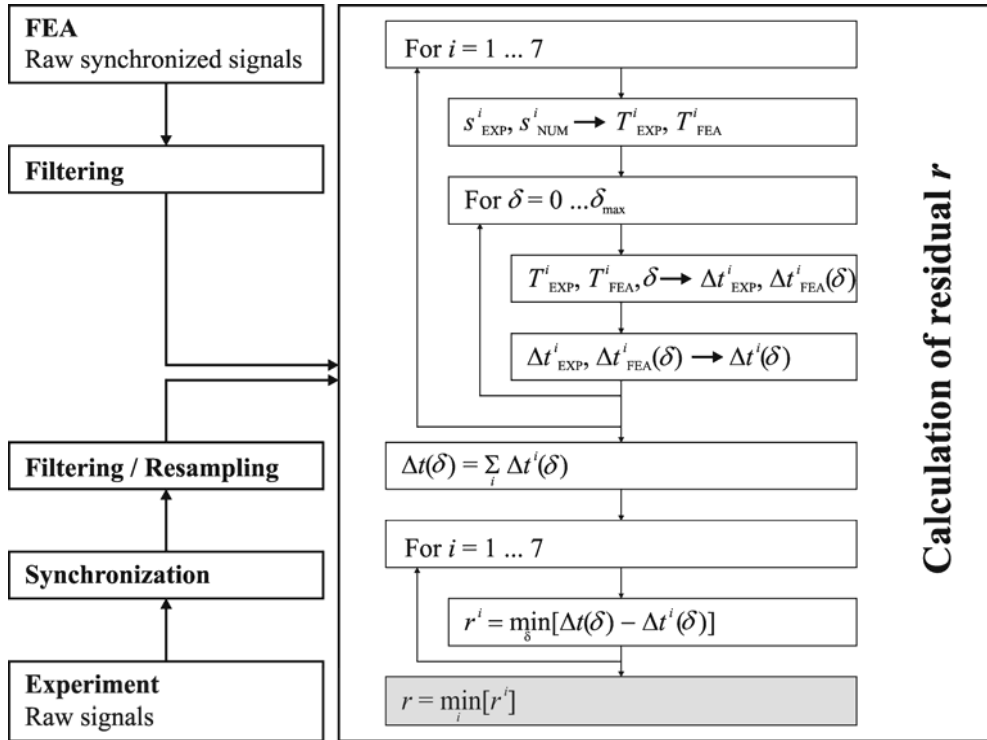
Figure 8. Flow chart of the residual calculation process.

The calculated residuals can be for single velocity value described by a surface. The influence of impact velocity is negligible on the surfaces calculated with the use of triggers (4) and (5) but it is not smooth enough for the use of the gradient method. Therefore, the evolution strategy with settings given in Figure 9 was used. The results of the evolution strategy are shown in the following Figures 10 to 13 with necessary details.
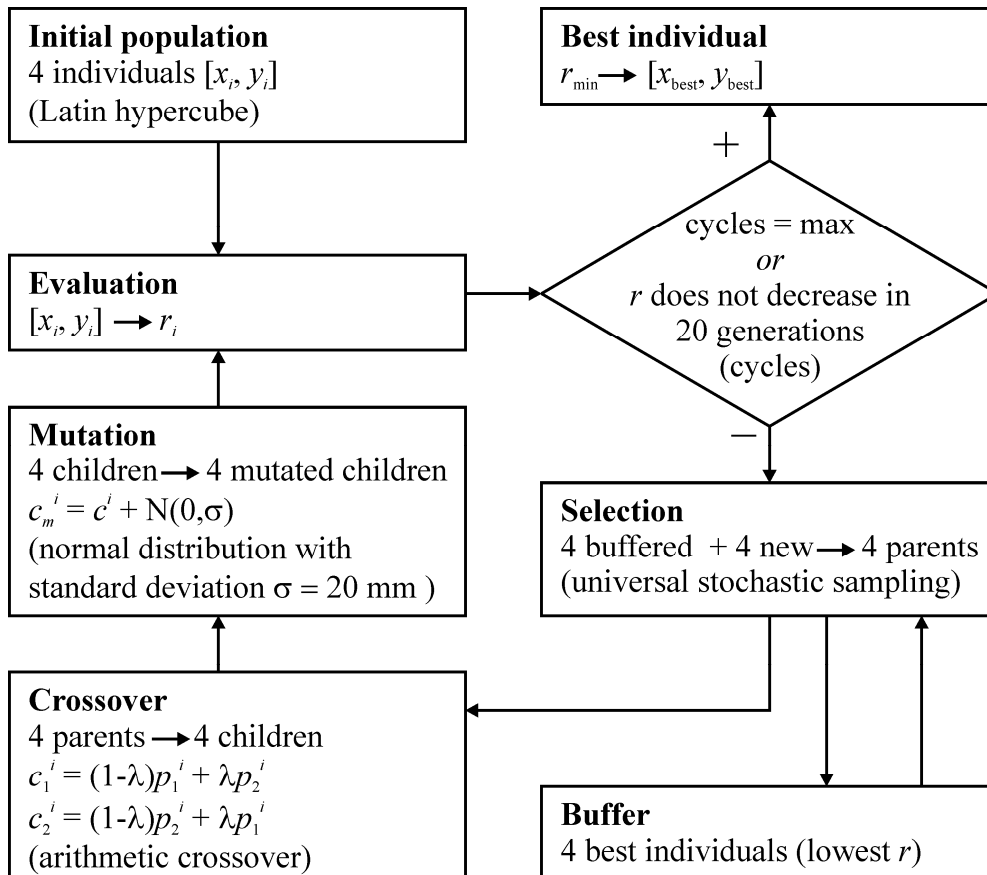
3-3. COMPARISON OF THE METHODS

Table 2 presents the comparison of accuracy of identification for the two chosen methods. The time consumption of the ray method methods is in seconds while there are approximately 50 identification steps in FEA based method each of which takes several minutes. The advantage of the latter method is the accuracy and the possibility to carry out subsequent post-processing such as failure analysis.

Table 2. Errors of both methods for different impact positions. Errors are given in element edge length a = 5 mm.

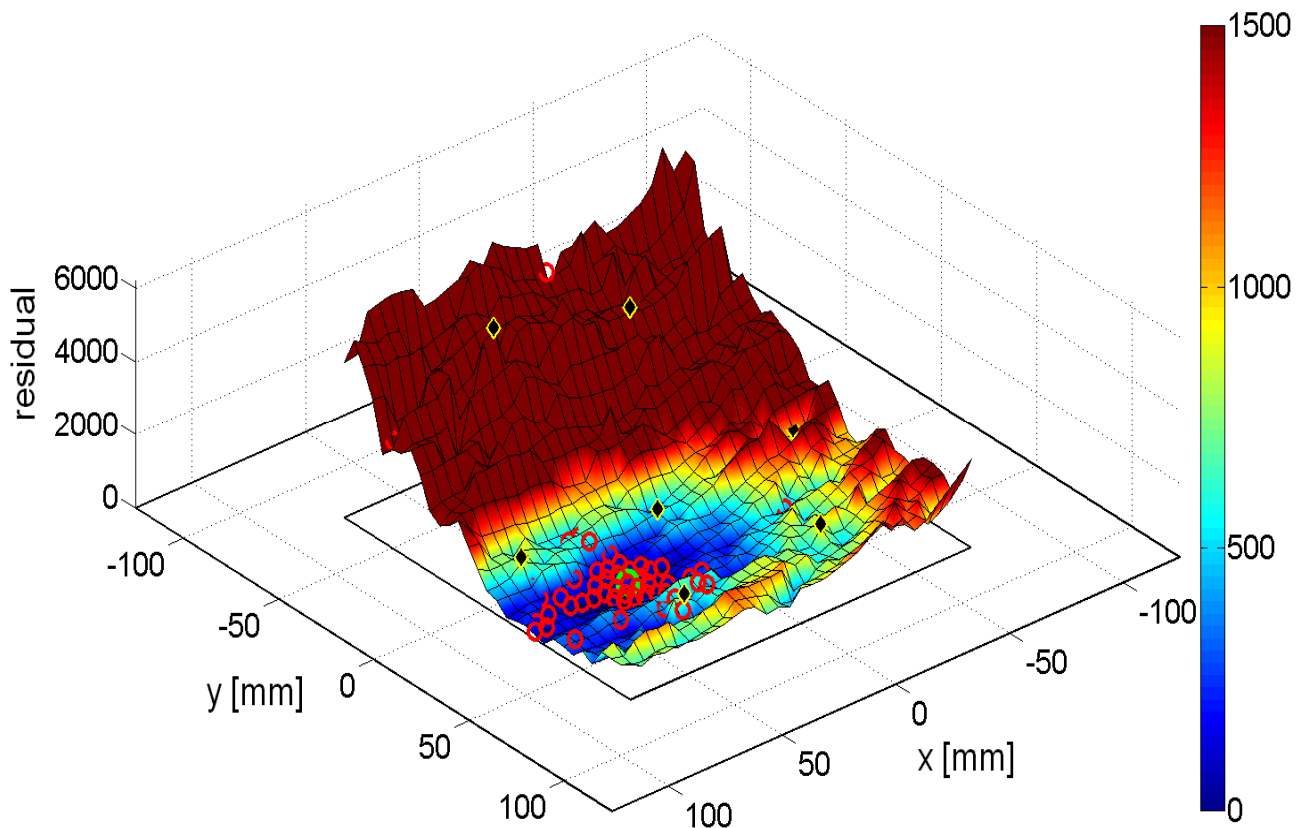| x [mm]	y [mm]	Ray method [$x/a \times y/a$]	FEA based method [$x/a \times y/a$]
0	0	0×0	2×1
60	0	0×4	1×1
0	65	3×0	0×1
20	10	1×0	0×0
50	50	3×3	1×0
30	20	1×1	0×1

Figure 10. Identification of impact position [x, y] = [50, 50] mm on virtual data, real residual surface (axes – plate, black small square – area of identification, black diamonds – strain gauges, red circles – identification steps, green circle – impact position).
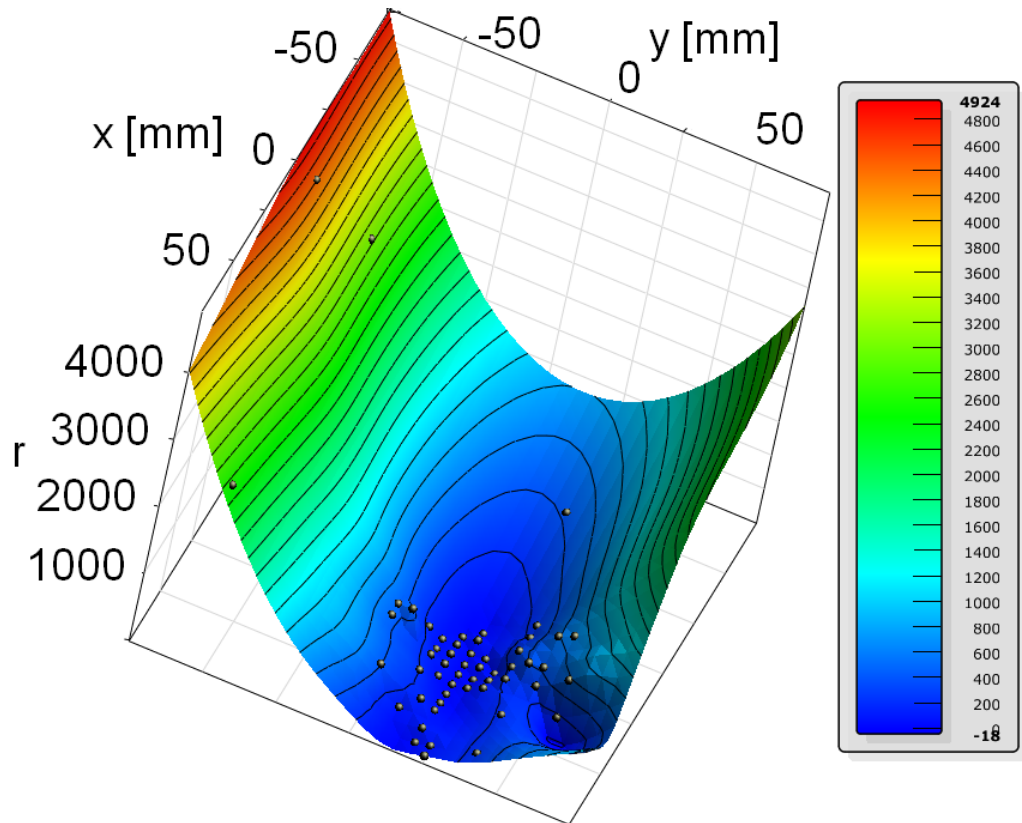
Figure 11. Identification of impact position [*x*, *y*] = [50, 50] mm on virtual data. Approximated residual surface taken from optiSLang (axes – area of identification, black dots – identification steps)
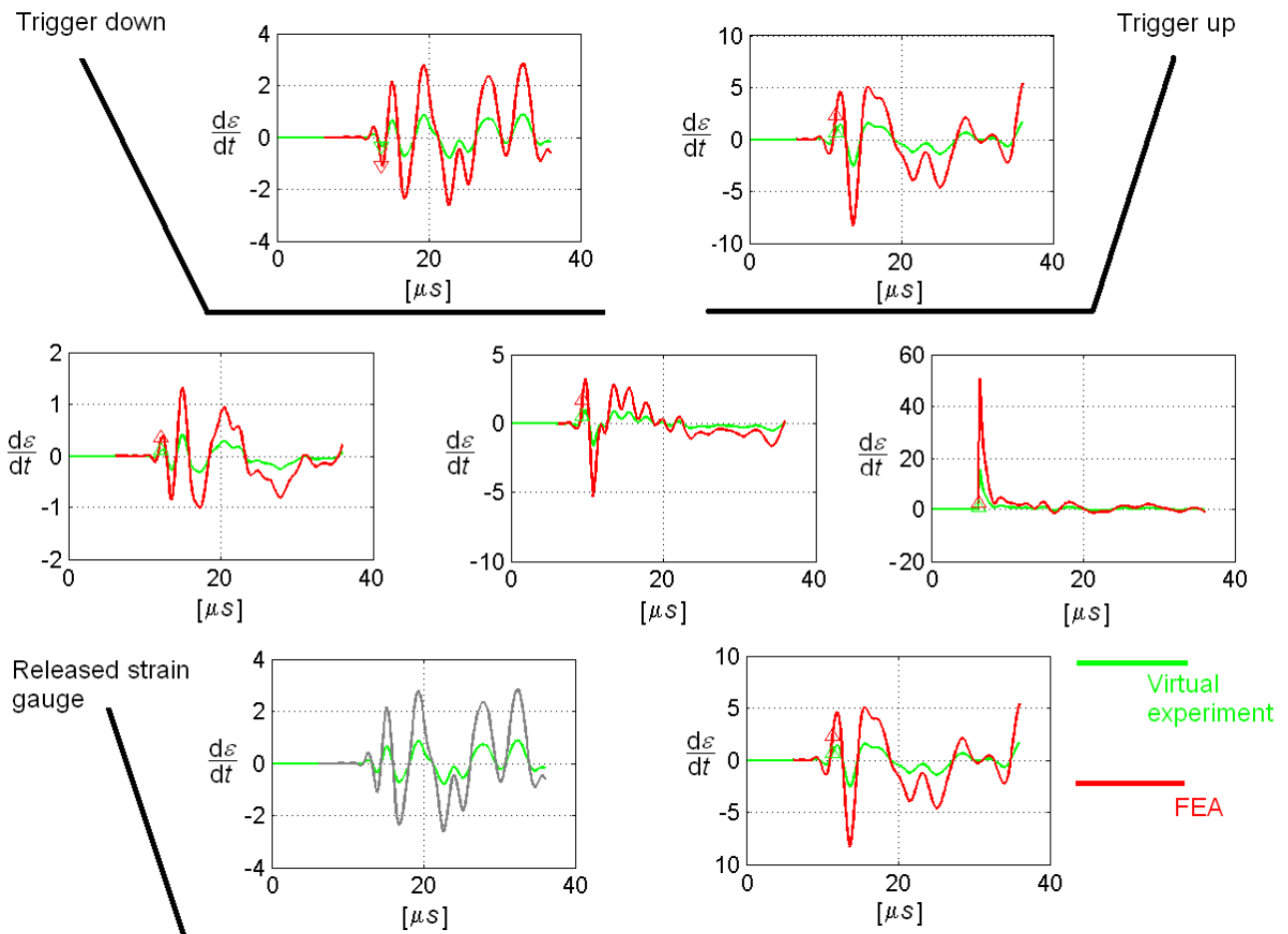

Figure 12. Comparison of the signals in identification of impact position [*x*, *y*] = [65, 0] mm. Both signals obtained from
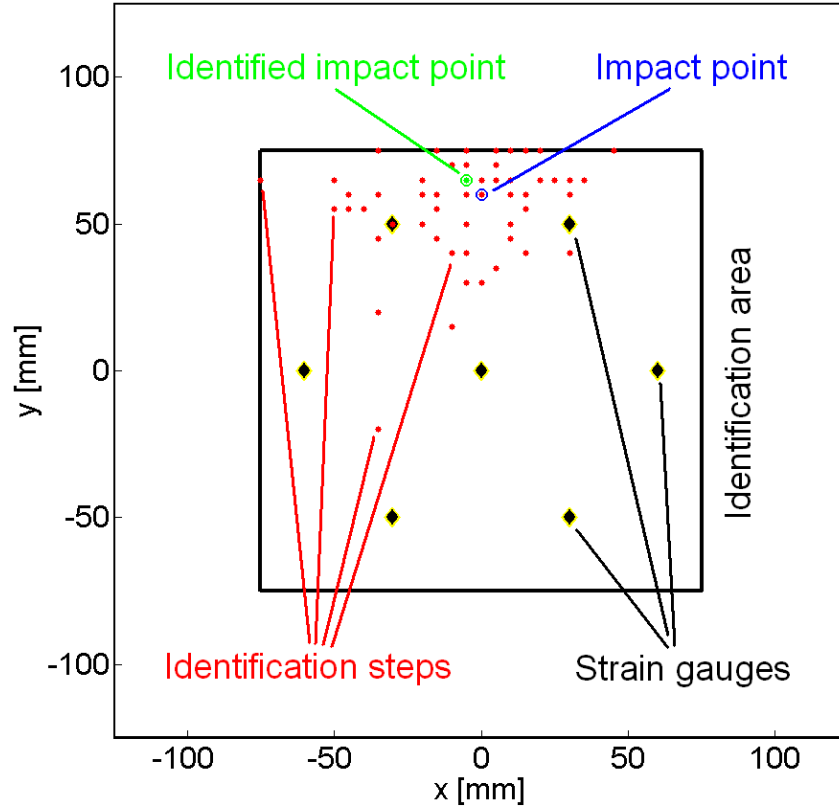
Figure 13. Identification of impact position on real experimental data $[x, y]$ = [0, 60] mm.

4. FAILURE ANALYSIS

An example of failure analysis which simulates the non-stationary state of stress of the plate for identified location of impact is performed. The FEA uses Puck's failure criterion [9], which belongs to so-called direct mode criteria, since it predicts the failure independently for different mechanisms or modes. The calculation of the failure indices *FI* is summarized in Table 3. The distribution of matrix failure index is displayed in Figure 14 for impact at x = 30 mm, y = 20 mm. The matrix failure is the most likely to occur in the investigated problem. The maximum value of matrix failure index was 0.104 while that of fiber was only 0.019 in this case.

The simulation of damage in case of higher impact energy will be performed in the forthcoming investigations using progressive failure analysis (PFA). This strategy was used on similar problem with composite plate [4]. For more complicated stress-state the LaRC04 criterion will be utilized. It was successfully implemented into MSC.Marc [4] and tested in the design of pin joints [5].

Table 3. Puck's action plane concept (for details see [8, 9]).

Mode	Failure condition	Condition of validity
(a)	$FI_{\mathrm{F}} = \dfrac{E_{\mathrm{L}}}{X^{\mathrm{T}}}\left(\varepsilon_{\mathrm{L}} + \dfrac{v_{\mathrm{f}}}{E_{\mathrm{f}}} m_{\sigma\mathrm{f}}\sigma_{\mathrm{T}}\right)$	$(...) \geq 0$
(b)	$FI_{\mathrm{F}} = -\dfrac{E_{\mathrm{L}}}{X^{\mathrm{C}}}\left(\varepsilon_{\mathrm{L}} + \dfrac{v_{\mathrm{f}}}{E_{\mathrm{f}}} m_{\sigma\mathrm{f}}\sigma_{\mathrm{T}}\right)$	$(...) \leq 0$
(c)	$FI_{\mathrm{M}} = \sqrt{\left(\dfrac{\tau_{\mathrm{LT}}}{S^{\mathrm{L}}}\right)^{2} + \left(1 - p_{\perp\parallel}^{(+)}\dfrac{Y^{\mathrm{T}}}{S^{\mathrm{L}}}\right)^{2}\left(\dfrac{\sigma_{\mathrm{T}}}{Y^{\mathrm{T}}}\right)^{2}} + p_{\perp\parallel}^{(+)}\dfrac{\sigma_{\mathrm{T}}}{Y^{\mathrm{T}}}$	$\sigma_{\mathrm{T}} \geq 0$

(d)
$$FI_{\mathrm{M}} = \frac{1}{S^{\mathrm{L}}}\left(\sqrt{\tau_{\mathrm{LT}}^2 + \left(p_{\perp\parallel}^{(-)}\sigma_{\mathrm{T}}\right)^2} + \left(p_{\perp\parallel}^{(-)}\sigma_{\mathrm{T}}\right)\right) \qquad \sigma_{\mathrm{T}} < 0,\ \left|\frac{\sigma_{\mathrm{T}}}{\tau_{\mathrm{LT}}}\right| \leq \frac{R_{\perp\perp}^{\mathrm{A}}}{\left|\tau_{\mathrm{LTc}}\right|}$$

(e)
$$FI_{\mathrm{M}} = \left[\left(\frac{\tau_{\mathrm{LT}}}{2\left(1 + p_{\perp\perp}^{(-)}S^{\mathrm{L}}\right)}\right)^2 + \left(\frac{\sigma_{\mathrm{T}}}{Y^{\mathrm{C}}}\right)^2\right]\frac{Y^{\mathrm{C}}}{-\sigma_{\mathrm{T}}} \qquad \sigma_{\mathrm{T}} < 0,\ \left|\frac{\tau_{\mathrm{LT}}}{\sigma_{\mathrm{T}}}\right| \leq \frac{\left|\tau_{\mathrm{LTc}}\right|}{R_{\perp\perp}^{\mathrm{A}}}$$

with $\quad R_{\perp\perp}^{\mathrm{A}} = \dfrac{Y^{\mathrm{C}}}{2\left(1 + p_{\perp\perp}^{(-)}\right)}$, $\ p_{\perp\parallel}^{(+)} = p_{\perp\parallel}^{(-)} = p_{\perp\perp}^{(-)}\dfrac{S^{\mathrm{L}}}{R_{\perp\perp}^{\mathrm{A}}}\ $ and $\ \tau_{\mathrm{LTc}} = S^{\mathrm{L}}\sqrt{1 + 2p_{\perp\perp}^{(-)}}$

where $\ E_{\mathrm{f}} = 230$ GPa and $\nu_{\mathrm{f}} = 0.18$ (taken from manufacturer), $m_{\sigma\mathrm{f}} = 1.2$ and $p_{\perp\perp}^{(-)} = 0.2$

5. CONCLUSIONS

Experimental analysis of non-stationary state of stress of unidirectional carbon/epoxy composite plate induced by impact of glass projectile was performed. Seven semiconductor strain gauges applied in a hexagonal pattern were used to record the strain rate. The signals from oscilloscopes were then post-processed. Two methods were used to identify the location of impact using the knowledge of wave front arrivals. The first method used ray tracking, while the latter was a combination of finite element analysis and mathematical optimization. The ray method proved to be much faster but less accurate. Moreover, the finite element based method can serve as the base for subsequent failure analysis. The authors expect to further extend this methodology by the damage estimation for cases with higher energy impacts.
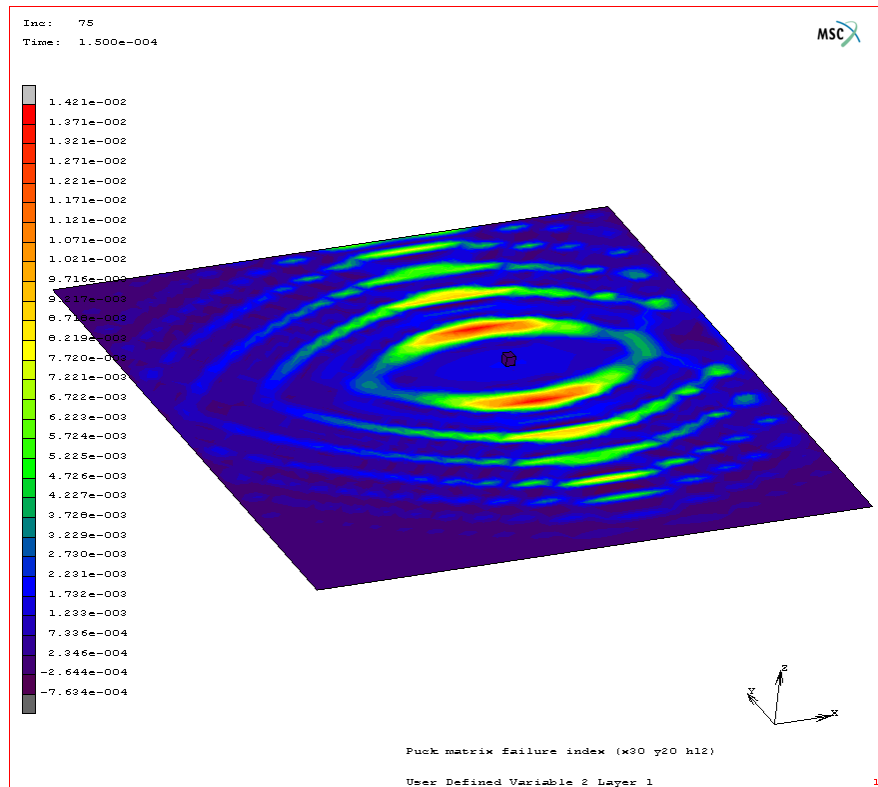

Figure 14. Example of space distribution of matrix failure index.

ACKNOWLEDGEMENTS

REFERENCES

1. Advancements and Challenges for Implementation: Structural Health Monitoring 2005. Edited by Fu-Kuo Chang, DEStech Publications Inc., 2005.
2. Berthelot J.-M.: Composite materials, Mechanical behavior and structural analysis. Springer, Berlin, 1998.
3. Damage Prognosis: For Aerospace, Civil and Mechanical Systems. Edited by D. J. Inman, C. R. Farrar, V. Lopes Jr., V. Steffen Jr., John Wiley & Sons, 2005.
4. Kottner, R.: Joining of Composite and Steel Machine Parts with Special Focus on Stiffness and Strength (in Czech). Doctoral thesis, University of West Bohemia, Plzeň, 2007.
5. Kroupa, T.: Damage of composites due to impact (in Czech), Doctoral thesis, University of West Bohemia, Plzeň, 2006.
6. Kroupa, T., Laš, V.: Off-axis behavior of unidirectional FRP composite, In: 15th Conference on Materials and Technology, Materials and Technology 3(42), ISSN 1580-2949, pp. 125–129, 2007.
7. Proceedings of the Third European Workshop: Structural Health Monitoring 2006. Edited by Alfredo Guemes, DEStech Publications Inc., 2006.
8. Puck A., Kopp J., Knops M.: Guidelines for the determination of the parameters in Puck's action plane strength criterion. Composites Science and Technology, 62, pp. 371–378, Elsevier, 2002.
9. Puck A., Schürmann H.: Failure analysis of FRP laminates by means of physically based phenomenological models. Composites Science and Technology, 58, pp. 1045–1067, Elsevier, 1998.